Engineering Science and Technology, an International Journal xxx (xxxx) xxx

HOSTED BY

Contents lists available at ScienceDirect

Engineering Science and Technology, an International Journal

journal homepage: www.elsevier.com/locate/jestch

Full Length Article

Effects of CuO, TiO_2 and graphite microparticles on the heat transfer properties of greases

Gokhan Gokdemir [a,1,*], Nimeti Doner [a,*], Zerrin Sert [b,2], Fatih Sen [c,3], Kerem Ciddi [d,4]

[a] Gazi University, Mechanical Engineering Department, 06570 Ankara, Turkey
[b] Eskişehir Osmangazi University, Mechanical Engineering Department, 26040 Eskisehir, Turkey
[c] Kutahya Dumlupinar University, Biochemistry Department, Sen Research Group, 43270 Kutahya, Turkey
[d] Kutahya Dumlupinar University, Industrial Engineering Department, 43270 Kutahya, Turkey

ARTICLE INFO

Article history:
Received 28 March 2021
Revised 10 July 2021
Accepted 2 August 2021
Available online xxxx

Keywords:
Grease
Microparticles
Temperature distribution
Absorption
Radiative properties
DDA

ABSTRACT

Heavy machinery operating in outdoor environments is exposed to both solar radiation and intensive load-bearing during operation. The long operating life of these machines and their components is enabled by the greases used in their bearings. The thermal properties of these greases play a crucial role in dissipating both the heat generated by friction in the bearings and the heat absorbed via solar radiation. In this study, we focus on maintaining successful heat transfer management in these machines. We select two types of grease, thickened with lithium and caoutchouc, containing CuO, TiO_2 and graphite microparticles at 0.02, 3.33 and 10 wt%., respectively, which are used as additives to improve the heat transfer effects. A test rig is prepared to investigate the changes in temperature and torque under real operation conditions. The radiative properties of the non-additive greases are examined in the ultraviolet-visible range, and the greases with additives are examined over a wavelength range of 2.5–20 μm. The absorption properties of the greases are numerically determined based on the discrete dipole approximation for two different values of the imaginary part (k) of the complex refractive indices ($m = n + ki$) of the additive materials. Uncertainty analyses of the experimental results were performed using SPSS software. The temperature and torque distributions varied according to the weight fraction of the metallic microparticles and the type of grease, with the caoutchouc-thickened grease reaching higher temperatures and torques than the lithium-thickened grease. The temperature distributions of the lithium-thickened grease with additives were lower than for the same grease with no additives, while the temperature distributions of the caoutchouc-thickened grease with additives were higher than those for the same grease with no additives. The absorption values of the greases containing additives were lower than for samples with no additives in the infrared wavelength spectrum, except for a mixture of graphite and TiO_2 at 10 wt%. The added microparticles positively influenced the heat transfer management of the greases.
© 2021 Karabuk University. Publishing services by Elsevier B.V. This is an open access article under the CC BY-NC-ND license (http://creativecommons.org/licenses/by-nc-nd/4.0/).

1. Introduction

Greases are used to reduce friction and wear problems in mechanical systems that require special solutions under certain operating conditions, such as high temperatures, high loads and low operating speeds [1,2]. The machines used for laying roads in outdoor environments, such as bulldozers, excavators and graders, are exposed to sunlight during the day. Of the components of solar radiation, 5% are in the ultraviolet (UV) range, 43% the visible range and 52% in the infrared wavelength range [3]. This means that heavy machinery is exposed to radiation at visible and infrared wavelengths during its period of operation, and the absorption of solar radiation at these specified wavelengths results in additional heat effects in the bearings of these machines. It is therefore necessary to minimise absorption in the visible and near-infrared wavelength spectra in order to reduce the problem of heating of machines operating outdoors.

The contents and thermal properties of greases vary according to their operating conditions and the industrial applications in

* Corresponding authors.
E-mail addresses: ggokdemir@kgm.gov.tr (G. Gokdemir), nimetidoner@gazi.edu.tr (N. Doner), zbocu@ogu.edu.tr (Z. Sert), fatih.sen@dpu.edu.tr (F. Sen), kerem.ciddi@dpu.edu.tr (K. Ciddi).
Peer review under responsibility of Karabuk University.
[1] ORCID: 0000-0002-6811-6849.
[2] ORCID: 0000-0001-6934-5443.
[3] ORCID: 0000-0001-9929-9556.
[4] ORCID: 0000-0002-8080-8725.

https://doi.org/10.1016/j.jestch.2021.08.001
2215-0986/© 2021 Karabuk University. Publishing services by Elsevier B.V.
This is an open access article under the CC BY-NC-ND license (http://creativecommons.org/licenses/by-nc-nd/4.0/).

Please cite this article as: G. Gokdemir, N. Doner, Z. Sert et al., Effects of CuO, TiO_2 and graphite microparticles on the heat transfer properties of greases, Engineering Science and Technology, an International Journal, https://doi.org/10.1016/j.jestch.2021.08.001

which they are used [4]. Greases consist of thickeners, base oils and additives, and they are named based on the thickener. The film thicknesses of greases are determined by the thickener, and their performance is affected by the structure of this thickener [5]. Lithium-thickened grease is used worldwide in mechanical systems for heavy load-carrying and high-speed applications due to its applicability over a broad range of temperatures, while caoutchouc-thickened grease is mostly used in mechanical systems with medium and light load-carrying applications due to its water-resistant properties and low cost [6,7]. The temperature distribution and the absorptivity or transmissivity properties of semi-solid lubricants such as greases affect their properties, including viscosity and load resistance, in the bearings of machines.

A study performed by Prasad et al. involved the addition of various metallic microparticles to a lubricant mixture and an examination of the temperature changes over a long operating period [8]. In another study, the addition of nanoparticles (Si, SiO_2, Al, Al_2O_3, Cu and CuO) to lubricants was numerically studied [9] and it was determined that the viscosities of the lubricants containing nanoparticles were highly dependent on the temperature. As discussed in a review study of the thermal characteristics of lubricants with added nanoparticles performed by Goal et al. [10], the bearing capacity was increased and the friction forces and contact areas between contacting surfaces were decreased. Peña-Parás et al. [11] studied the effect of temperature on the extreme pressure on CuO and TiO_2 nanoparticle-filled lubricants and found a reduction in the contact area of moving surfaces and an increase in the load-carrying capacity. The thermal conductivity and lubricity for nanogrease with added carbon nanotubes were studied by Hong et al. [12], who reported that the thermal properties could be improved by changing the homogeneity and weight fraction of the nanoparticles. In another study, the effects of temperature and viscosity on the performance of lubricants made with graphite-added grease were investigated and it was found that the viscosity decreased as the temperature increased [13].

Lubrication with grease is accomplished by the distribution of the thickening property of long fatty acid chain soaps, with materials such as lithium, sodium and calcium. Sodium- and calcium-thickened greases have been replaced by lithium-thickened greases due to their multifunctional properties and long usage times [14]. The absorption properties of lithium-based grease at low temperatures were investigated by Zhou et al. [15], and the thermal conductivity, friction and load resistance of greases with additive nanoparticles (TiO_2, Al_2O_3, CuO and multi-walled carbon nanotubes) for mechanical systems were investigated in detail by Peña-Parás et al. [16,17]. These authors studied two different nanogreases with mixes of 0.01, 0.05 and 0.1 wt%, and concluded that nanogreases could be used to give good thermal and tribological performance. Similar studies of the conductive heat transfer of greases [18] and their properties have been presented [19]. However, the number of studies that have considered solar radiation when examining the thermal and flow properties of greases or nanofluids is very small. In one such study, the thermal behaviours of nanofluids exposed to solar radiation were investigated numerically by Kandasamy et al. [20]. These authors found that the temperature, nanoparticle volume fraction and flow field were all highly affected by solar radiation, and that the flow properties were changed. In two other studies, the thermal performance of solar collectors using nanofluids exposed to solar radiation and the optical properties of nanofluids were evaluated [21,22].

Due to a lack of studies of the absorption properties of greases with added microparticles, and to prepare an effective heat transfer phenomenon for machines operating in outdoor environments, we focus here on the temperature distributions and the radiative properties of additive and non-additive greases. The samples used in our study were greases with codes 51502-KP 2K-20 and 51825-KP 2 E-10 based on the DIN standards. The first code represents Grease 1, which was thickened with lithium, while the second represents Grease 2, thickened with caoutchouc, with a calcium base oil. These were selected as they are the most widely used types of grease in engineering applications. Three different additives (CuO, TiO_2 and graphite) were used with these two greases. An experimental test rig was prepared to simulate the real operating conditions of a bearing, and the changes in temperature and torque over time were investigated. The absorption properties of the greases with and without additives were measured and numerically evaluated for the first time in the literature, using discrete dipole approximation (DDA). The effects of the imaginary part (k) of the complex refractive index of the microparticles on the optical properties of the greases were also analysed.

2. Experimental

2.1. Temperature measurements

Temperature measurements were performed for greases containing microparticles and non-additive greases using the test rig shown in Fig. 1. The wear jaw generated frictional heat, leading to a horizontal temperature gradient, as the test plate was actuated by an asynchronous 450 V three-phase electric motor with 0.25 kW power and a rotating speed of 1390 rpm. A reduction gear with a 7.5/1 ratio was used, which changed the motion by 90° at the exit of the motor. For the rotational movement, a 30 kg load was applied and the movement was transmitted to the test pieces via the reduction gear at an average of 185 rpm, and the torque was increased by an average factor of 7.5. A hole 5 mm in diameter was drilled along the axis of the wear jaw shaft and the grease to be tested was transferred to the friction medium through this channel. The temperature was measured by two sensors placed on the wear plate and was evaluated by taking the average value. The accuracy of measurement was verified by checking with a laser thermometer (model: Sinometer BM380; Fig. 1(b)) that was repeatedly calibrated during each experiment process. The load was measured with a load cell and sent to an electronic control card. The measurement of this value was critical to ensure that comparisons were made under the same conditions. The wear plate was made of a brass-bronze material, and was 80 mm in diameter and 5 mm thick. Since this material is used as a bearing material in many mechanical applications, it was chosen to provide real operating conditions. The electronic control unit used an Arduino Uno-type programming board and electrical conductors to control the three-phase motor. The rotation time and direction of the electric motor were controlled via these contactors. When the test rig had been prepared, the experiment was started by pressing the start button. The wear jaw was first rotated clockwise and counter-clockwise at regular intervals. The test rig was operated until a set number of repetitions was reached, and the load, moment, temperature, and repetition numbers were recorded during the tests (at intervals of 24 s). The electronic programming card processed the data received from the temperature and load sensors and sent it to the LCD monitor on the control unit and the computer. The tests were conducted for 60 min at a constant speed at a temperature of 25 °C and at the same pressure.

2.2. Absorption measurements

Absorbance can be characterised based on the experimental results for the transmittance and reflectance, and depends on the wavelength. Another feature that defines the optical properties of materials is the complex refractive index ($m = n + ki$), which involves two parameters: a real part, n, and an imaginary part, k.

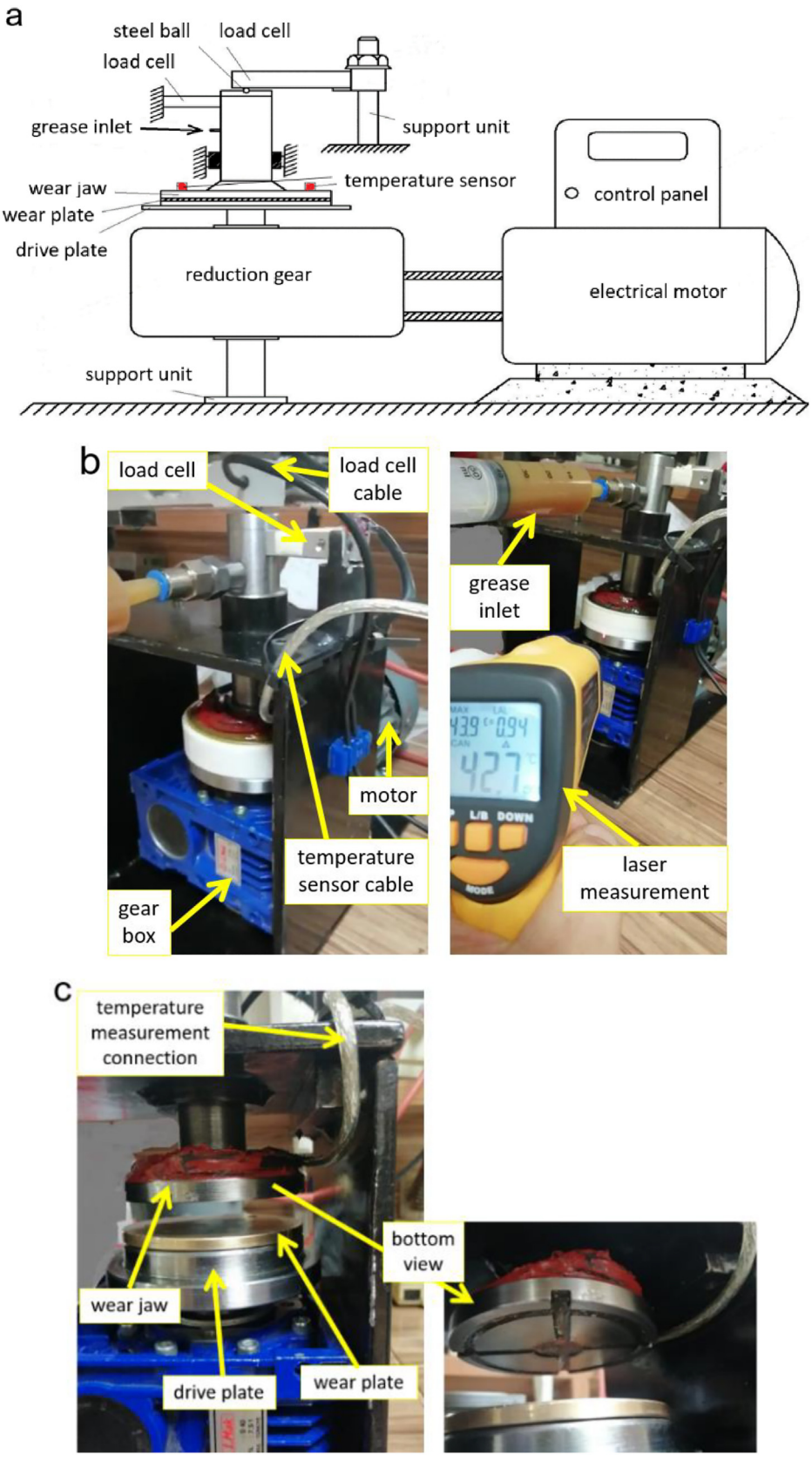


Fig. 1. (a) Schematic and (b) photographic views, and (c) the wear jaw of the test rig.

These two parameters become more important in determining the scattering behaviour as the wavelength changes [23]. In addition, when radiation penetrates a medium, including rigid particles, the beam of radiation is absorbed or reflected by the particles.

The loss in intensity of the radiation due to absorption as light travels through the medium is given by the Beer-Lambert law [3], defined as in Eq. (1):

$$\frac{I}{I_0} = e^{-L\kappa_{total}} \tag{1}$$

where L is the medium depth (cm), I_0 and I are the intensities of radiation at the surface and in the medium (W/m^2), respectively, and κ_{total} is the sum of the absorption coefficients of the particles (κ_{par}) and the grease (κ_{base}). Absorption measurements in the UV–visible spectrum are used to determine the amounts of organic and inorganic substances. Molecular absorption spectroscopy is based on measurements of the transmissivity (T) or absorbance (A) of a solution in a transparent container with a beam path at wavelength λ:

$$A = -\log T = \log\frac{I_0}{I_\lambda} = \varepsilon\lambda c \tag{2}$$

where I_λ is the intensity at wavelength λ (μm), ε is the molar absorption coefficient and c is the molar concentration. The indices m of metals are affected when their electrical resistivity (r_e) is small, and for long wavelengths ($\lambda_0 > 5$ μm), and the emissivity property (ε) can be predicted by the Hagen-Rubens relation. The absorption is then calculated as $1 - \varepsilon$, based on Kirchhoff's law and the reflectivity reciprocity relations [3]:

$$\varepsilon_\lambda = \frac{2}{\sqrt{0.003}}\left(\frac{r_e}{\lambda_o}\right)^{1/2} - \frac{2}{0.003}\frac{r_e}{\lambda_o} \tag{3}$$

In this study, the absorbance measurements were performed with two different spectrophotometer devices. A PerkinElmer Lambda 750 spectrophotometer was used for absorbance measurements in the UV–visible wavelength range at room temperature. For these measurements, 2 mg of the greases were diluted with 2 mL of hexane using a vortex mixer for 30 min to obtain a homogeneous solution. Reference measurements for hexane were performed for the device and the diluted greases were then measured. To carry out absorbance measurements over a range of wavelengths of 2.5–20 μm, the greases and the microparticles were then mixed manually for 30 min at room temperature until well dispersed, as observed by the naked eye, and were then sequentially measured without delay using a PerkinElmer Spectrum Two spectrophotometer. All absorbance measurements were performed at least three times, and showed good repeatability.

Since CuO, TiO_2 and graphite are birefringent materials, the values of their complex refractive indices are essential for an understanding of absorption–scattering behaviours. CuO has high optical absorption, high-temperature superconductivity and a non-toxic structure [24–26]. Graphite has excellent lubrication characteristics [27,28], while TiO_2 has a large complex refractive index and transparency in the visible spectrum [29,30]. Due to these properties, CuO, graphite and TiO_2 were selected as additives for the greases in this study. The micromaterials were purchased from Sigma-Aldrich and the properties of the additive materials are shown in Table 1.

3. Numerical modelling of optical properties: The discrete dipole approximation

DDA is a valuable method for modelling light scattering [31], and is considered to be numerically exact [23,32]. The effects of light incident upon a particle are the sum of the reflection, refraction and absorption properties. This method computes the radiative properties of a particle or aggregate with the DDSCAT code, using Q (unitless) terms known as the particle extinction, scattering or absorption efficiency factors. In addition, the code uses data such as the complex refractive index, wavelength and the volumetric-equivalent effective radius ($\alpha_{eff} = N^{1/3}\alpha$), where N is the number of particles and α is the particle radius. DDA codes are publicly available, and use a target object with a number of dipoles located inside a Cartesian lattice and commonly used geometries, such as ellipsoids and rectangular and hexagonal prisms [33]. The polarisability of each dipole is a function of its effective volume and the optical constants of the target object. The absorption, scattering and extinction cross-sectional areas for a particle are defined as $C_i = Q_i\pi\alpha^2_{eff}$, where the subscript i represents absorption, scattering and extinction ($C_{ext} = C_{abs} + C_{sca}$). For the calculation of dipole polarisation, the DDA method requires a large number (N) of point dipoles that can interact between particles and the incident light, and the desired accuracy is taken as $|m|$ **kd** < 1, where **d** is defined as the lattice length, m is the reflection index and **k** is the wavenumber ($2\pi/\lambda$).

4. Results and discussion

Two kinds of grease used in bearings and wear zones were examined in terms of their heat transfer effects. Fig. 2 shows the X-ray diffraction (XRD) phases of the greases containing metal particles, before the investigation of the effects of the heat transfer properties was carried out. The XRD phases of the samples were characterised using a Rigaku diffractometer (Cu-Kα radiation) at a scanning rate of 0.005 2θ/min, with a power of 40 kV and 30 mA, over the range 5–80°. The morphological peaks characterising the added metal microparticles are visible in the XRD images in Fig. 2. In the case of the 0.02 wt% additive, the microparticles in the grease have only small morphological effects, except for TiO_2. Moreover, although the metallic particles and additive amounts were the same, it can be seen from Fig. 2 that there were some differences between the diffraction intensities in the XRD images based on the type of grease.

Our investigation of the heat transfer properties was carried out in two parts: first, the test rig was prepared and used to study the temperature and torque distributions, and following this, the effects of the addition of microparticles on the absorption properties of the greases were examined. To determine the effects of the quantity of additive, we used a minimum of 0.02 wt% and a maximum of 3.33 wt%. For the temperature and torque distributions, 20 mg and 3.33 g of microparticles (CuO, graphite and TiO_2) were added to 100 g of each grease, to give greases with weight fractions of 0.02 and 3.33 wt%. The experimental studies were repeated several times and stable results were obtained. The temperature curves obtained for the greases are given in Fig. 3. The temperature distributions for both greases increased at a high rate in the initial test procedure. This trend in the distributions was followed by a reduced rate of increase in the temperature over a longer test process. This change in temperature is consistent with the results of Prasad et al. [8]. The temperature distributions of Grease 2 with and without additives were higher than for Grease 1. Table 1 shows the thermal conductivities of the additive materials used, and it can be seen that TiO_2 has the lowest thermal conductivity while graphite has the highest. The thermal conductivity of CuO is also three or four times higher than that of TiO_2. Fig. 3 shows that although the thermal conductivities of the metallic additives are obviously different, the temperature distributions of the greases containing the additives both have similar parallel trends and are close to each other for each weight fraction. For 0.02 wt%, the temperatures of Grease 1 with additives over the first 20 min are ~ 5–6% lower than those for Grease 1 with no additives. After 40 min, the difference between them decreases to 2%. For the first 40 min of the tests, the temperature distributions of Grease 1 with additives are close to each other, and the temperatures of Grease 1

Table 1
Properties of microparticles.

Microparticles	Properties				
	Shape and size	Purity (%)	$m = n + ki$	Thermal conductivity (W/mK)	Electrical resistivity (Ω.cm)
CuO	Spherical, diameter < 5 μm	97	$m = 1.8 + 1.5i$ [24]	36 [26]	1.72×10^{-6} [39]
Graphite	Spherical, diameter < 20 μm	98	$m = 2.7 + 1.5i$ [35]	119–165 [28]	122×10^{-5} [40]
TiO_2	Spherical, diameter < 5 μm	98	$m = 3.5 + 1.5i$ [29]	8.4–11.2 [30]	39×10^{-6} [39]

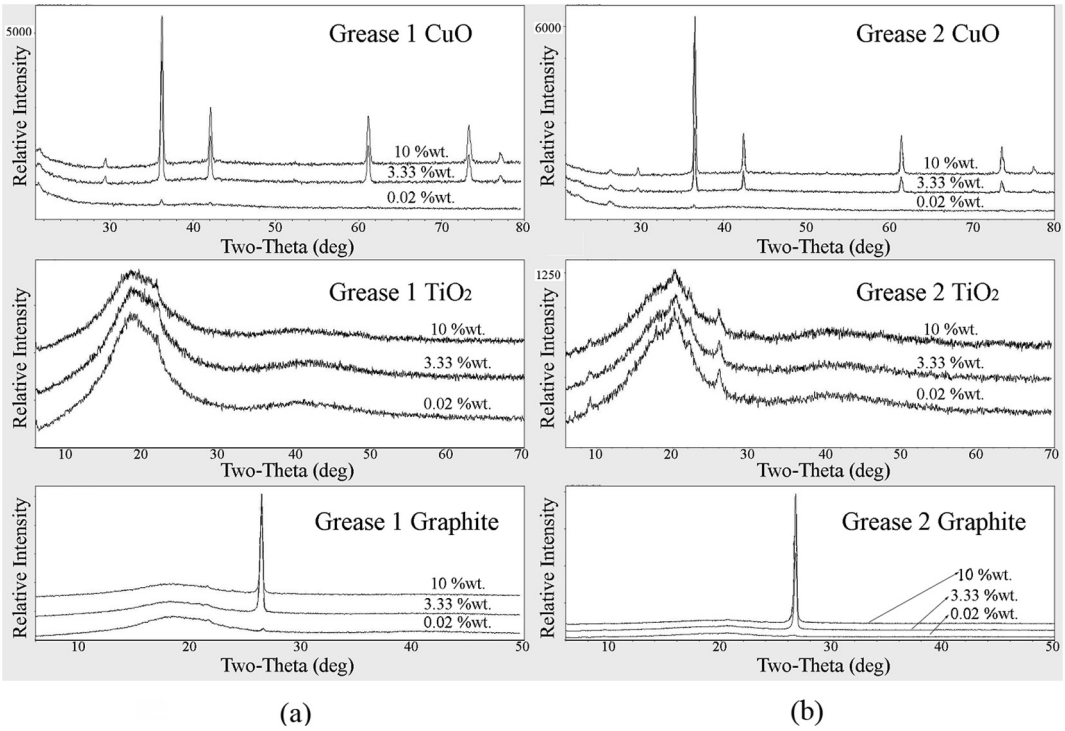


Fig. 2. XRD phases of greases with additives: (a) Grease 1; (b) Grease 2.

with CuO then increase rapidly. For Grease 2, the temperatures of the sample with additives over the first 20 min are ~ 10% higher than for Grease 2 with no additives. After 40 min, the difference between them is ~ 11%. The temperature values for Grease 2 with TiO_2 over the first 30 min are higher than for the others. Liquefaction was also observed in all investigated samples at the end of the experiments.

The torque curves for the greases with and without additives are presented in Fig. 4. After 10 min of the tests, the torque values for Grease 2 were higher than for Grease 1. From the results in Fig. 4, it can be seen that the torque values for Grease 1 with CuO were the lowest of all the samples for a weight fraction of 0.02 wt%; however, the torque values for the sample increased for a weight fraction of 3.33 wt%. The torque values for Grease 2 with CuO and graphite microparticles at 3.33 wt% were lower than for samples with a weight fraction of 0.02 wt%. These results show that the use of metallic additives is helpful in improving the heat and torque transfer mechanisms in bearings.

In the second part of the study, absorption measurements of the diluted greases (non-additive) were performed at UV–visible wavelengths, and images of the diluted greases and the measured absorption values are shown in Fig. 5(a) and (b), respectively. A significant peak in the absorption values for both greases can be observed at ~ 300 nm (0.3 μm), and it can be seen that the values for Grease 2 are higher than for Grease 1. An examination of the absorption measurements for non-additive greases at UV–visible wavelengths shows that the absorption values of both greases at wavelengths of > 0.4 μm are ~ 0.1. The maximum absorption values observed at 0.3 μm are eight times higher than for Grease 1 and 10 times higher than for Grease 2, based on the measured values for the greases in the wavelengths of > 0.4 μm. These absorption measurements are important for greases that are intended for use in machines operating in outdoor environments. We attempted to measure the absorption of grease with additives in the UV–visible spectrum, but these measurements could not be carried out due to sedimentation of the additives.

Samples of greases with additives at weight fractions of 0.02, 3.33 and 10 wt% were prepared in order to investigate the absorption properties in a wavelength range of 2.5–20 μm. Absorbance measurements can normally be made even for a small number of samples; however, for our experiments on the temperature and torque, a larger number of samples was needed due to the operating conditions of the test rig and the necessity of repeating the experiments several times. To determine the effects of the concentration of the additives on the heat transfer properties of a particular grease mixture, we also studied the changes in the absorbance of the grease mixtures up to a value of 10 wt% additive as an extreme case. From a survey of the literature, we did not any earlier studies of grease mixtures containing additives at 10 wt%, and we therefore performed the absorbance measurements of the samples at this concentration in order to observe the results for an extreme case and to obtain a benchmark result for comparison. However, due to the limited availability of metallic microparticles, we were unable to investigate the changes in temperature and

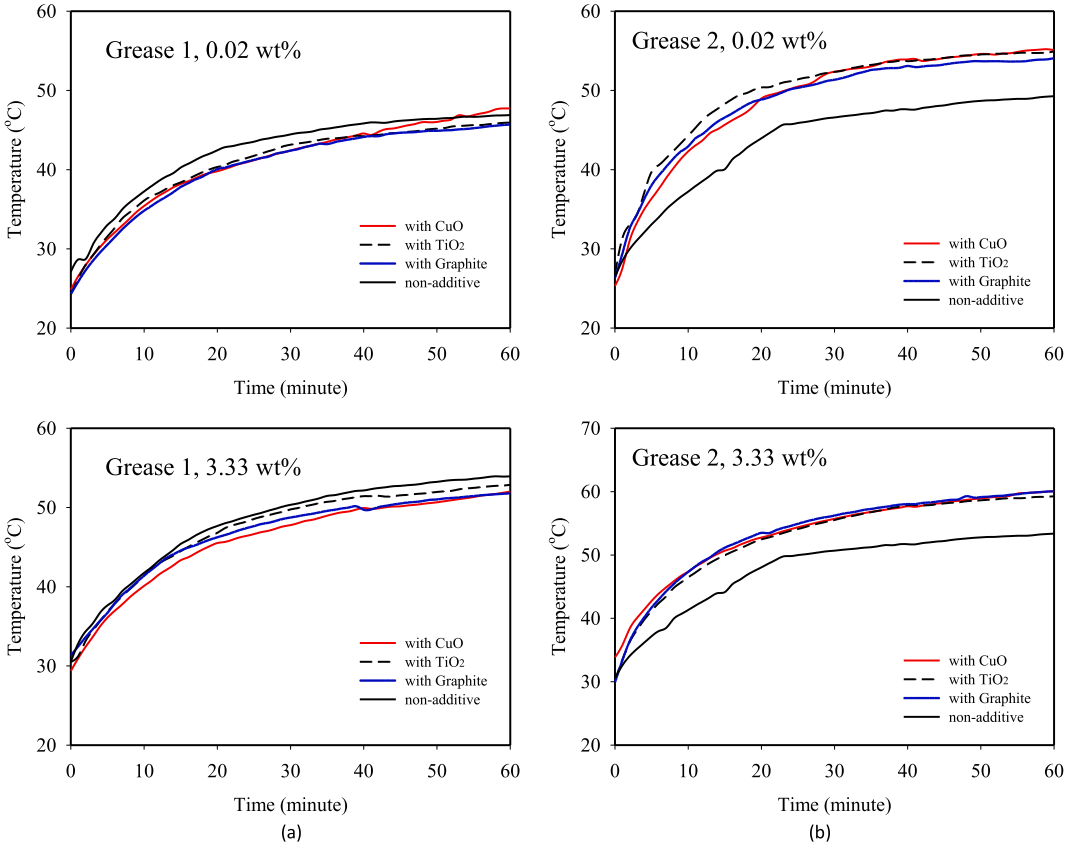


Fig. 3. Temperature curves for greases with and without additives: (a) Grease 1; (b) Grease 2.

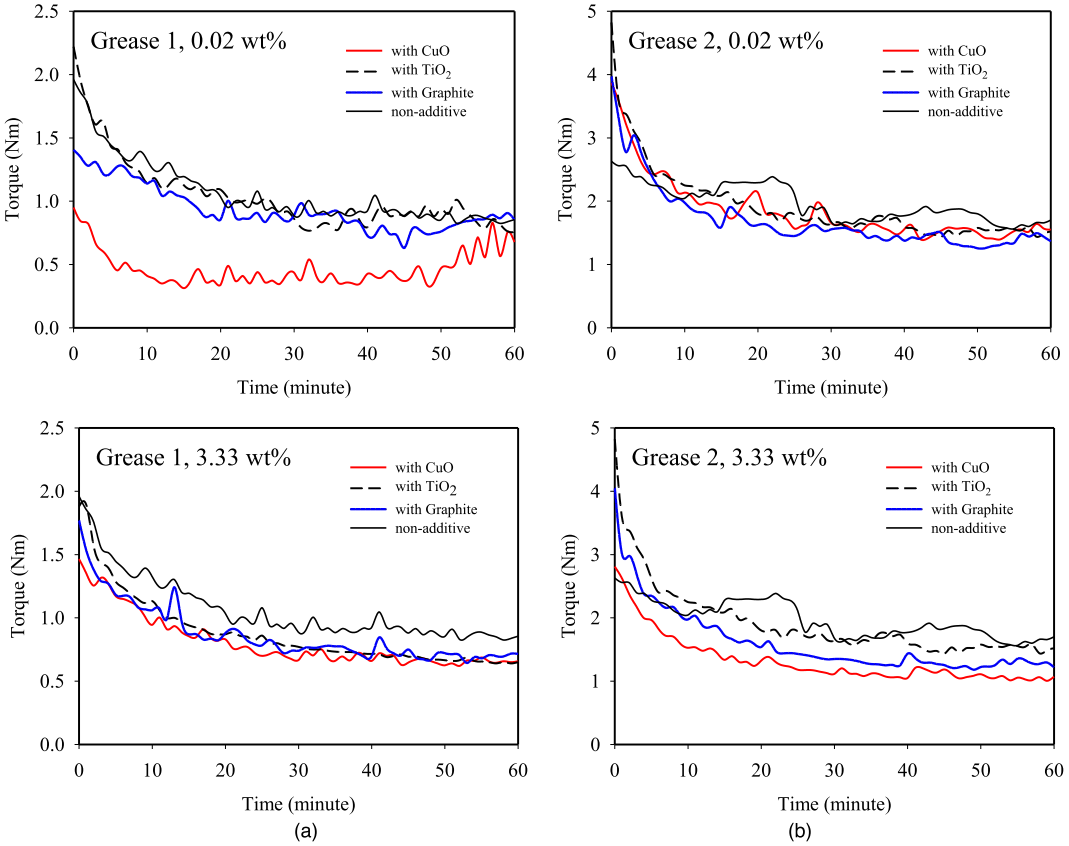


Fig. 4. Torque distributions for greases with and without additives: (a) Grease 1; (b) Grease 2.

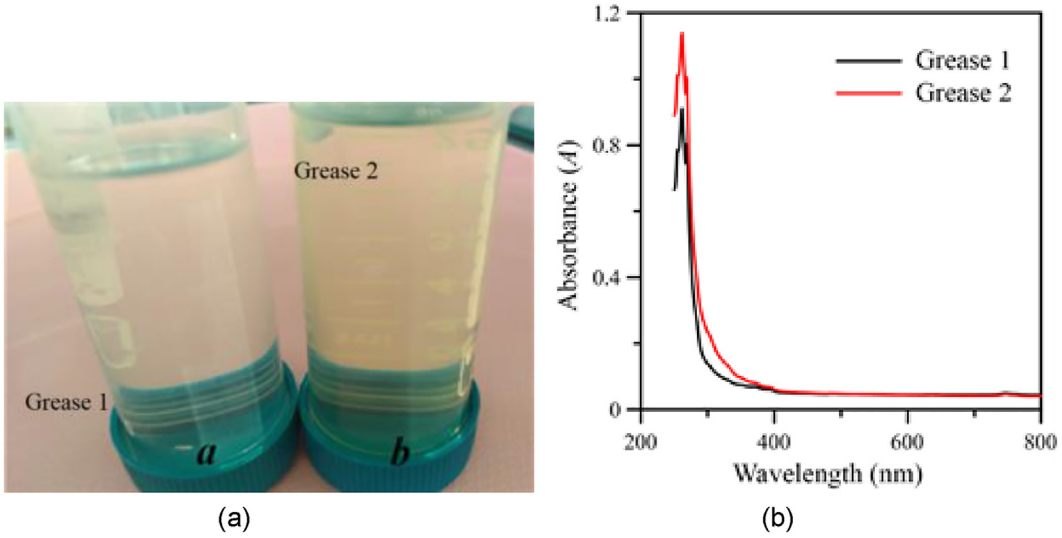


Fig. 5. (a) Images of grease samples and (b) absorption measurements in the UV–visible spectrum.

torque for samples with 10 wt% of additives. The absorption values for Grease 1 with additives at 0.02, 3.33 and 10 wt% are given in Fig. 6(a)–(c), respectively. The absorption values for Grease 1 without additives over a range of wavelengths of 2.5–20 μm were significantly higher than for Grease 1 with additives, except for the grease containing graphite at 10 wt%. The latter case showed the highest absorption values, and the values for Grease 1 with TiO_2 at the same weight fraction were also significantly increased. The results of our absorption measurements were consistent with those of Kanazawa et al. [34], showing C—H bonds at ~ 3.4 μm and C═O bonds at ~ 6.5 μm for a lithium thickener. The absorption values for Grease 1 with graphite at 0.02 and 3.33 wt% were very close to those for Grease 1 without additives. The absorption values for Grease 1 with CuO and TiO_2 at weight fractions of 0.02 and 3.33 wt% were also similar. Grease 1 with graphite at 10 wt% gave the maximum values at all wavelengths investigated here, as can be seen from Fig. 6(c). This situation was especially observed both to the high amount of the additive and result from its high electrical resistivity with regard to CuO and TiO_2. The absorbance of graphite evaluated using the Hagen-Rubens relation was obviously obtained high at all wavelengths. Similar values for the absorbance were also observed for TiO_2 at wavelengths >12 μm. As the proportion of microparticles added to Grease 1 in the range increased, the absorption values near-infrared wavelength also increased.

The results of the absorption measurements for Grease 2 with the same weight fractions are shown in Fig. 7. It can be seen from Fig. 7(a) and (b) that at 0.02 and 3.33 wt%, the absorption values for Grease 2 are similar over the wavelength range 2.5–15 μm, and are lower than for Grease 2 without additives. The same trend in the measured absorption values can be observed for Grease 2 as for Grease 1, except at an additive rate of 10 wt%. Fig. 7(c) shows that in this case, the absorption values for Grease 2 are lower for Grease 2 without additives at wavelengths of < 12 μm. The values for Grease 2 with TiO_2 are highest at wavelengths of 13.5–20 μm, as a result of its high electrical resistivity. Absorption measurements for graphite with Grease 2 at wavelengths greater than λ = 12 μm did not show similar behaviour to that of Grease 1. The peaks formed by the C–H and C-O bonds at ~ 3.2 and ~ 6.7 μm, as discussed in Ref. [34], are also seen for Grease 2. The maximum absorption values are seen for Grease 2 containing graphite at 0.02 and 3.33 wt% and TiO_2 at 10 wt%, with a value of 3.2 μm. In addition, there is a peak in the absorption values at ~ 13.8 μm in the fingerprint region (a wavelength range of ~ 7.1–16 μm) for the greases examined here. These peak values are thought to originate from the nature of base fluid of the grease. A ripple structure is seen in the absorbance measurements in Figs. 6 and 7, in which the absorption increases with the wavelength. Nicoletti [9] showed that the decay in the viscosities of lubricants decreases due to the minimum generated heat in the bearing, including the lubricant with nanoparticles. The decrease in the absorption values of these greases indicates that they will not absorb radiation from the environment and will not convert it to heat. It therefore appears that the compact thermal effects on the bearings caused by heat from both friction and radiation from the outdoor environment can be eliminated or decreased by these grease lubricants, as discussed in Ref. [9].

4.1. Uncertainty analysis

In order to investigate whether there was a difference between the average temperature, torque and absorbance measurements for Grease 1, Grease 2 and the additive samples, an uncertainty analysis was carried out using SPSS 17.0 (Statistical Package for Social Sciences) software. The temperature, torque and absorbance values were treated as the dependent variables and the types of grease as independent variables, and one-way ANOVA tests were performed. Since the equality of variances was not ensured, by choosing Brown-Forsythe and Welch options and looking at the Robust Tests of Equality of Means, the mean differences between temperature, torque and absorbance were found to be significant at the 0.05 level. Tamhane's T2 test was used for a *Post Hoc* Multiple comparison of the average differences at a significance level of 0.05, since the equality of variances could not be ensured. It was found that the average differences in temperature, torque and absorbance were significant at the 0.05 level. The correlation between the temperature and torque variables for all of the samples was significant at the 0.01 level (two-tailed). This means that the correlation is strong and negative: as one increases, the other decreases. The average temperature changes for the greases without additives were similar. There was no difference between the average temperature values for Grease 1 with additives of 0.02 wt% samples and these had the lowest average temperatures. Grease 1 with CuO 0.02 wt% showed the lowest average torque.

The effects of the absorption properties of the microparticles were investigated via the experiments described above, and the

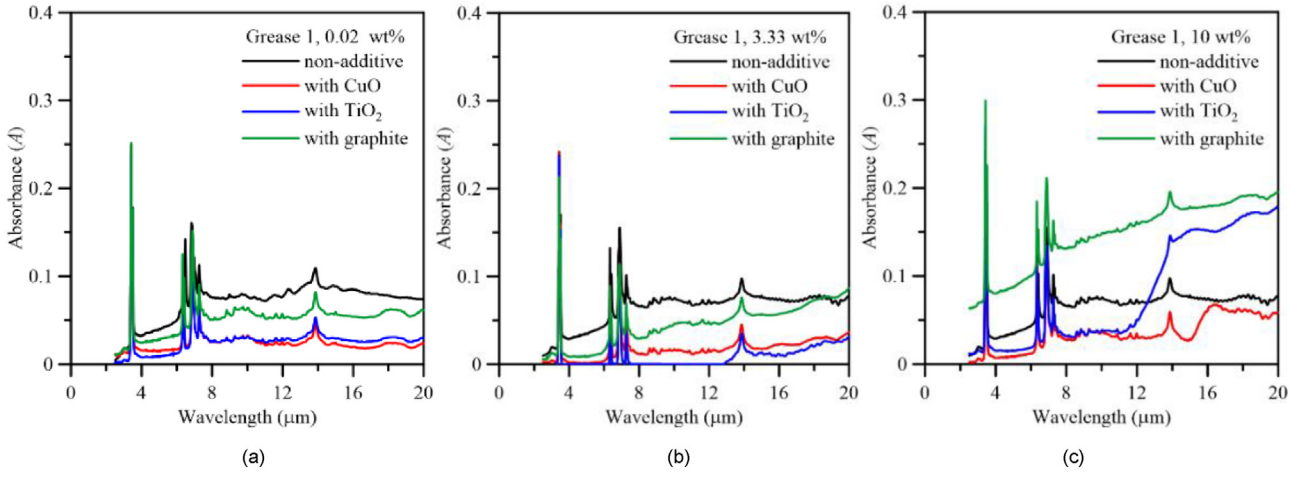


Fig. 6. Absorption measurements for Grease 1, with and without additives: (a) 0.02 wt%; (b) 3.33 wt%; (c) 10 wt%.

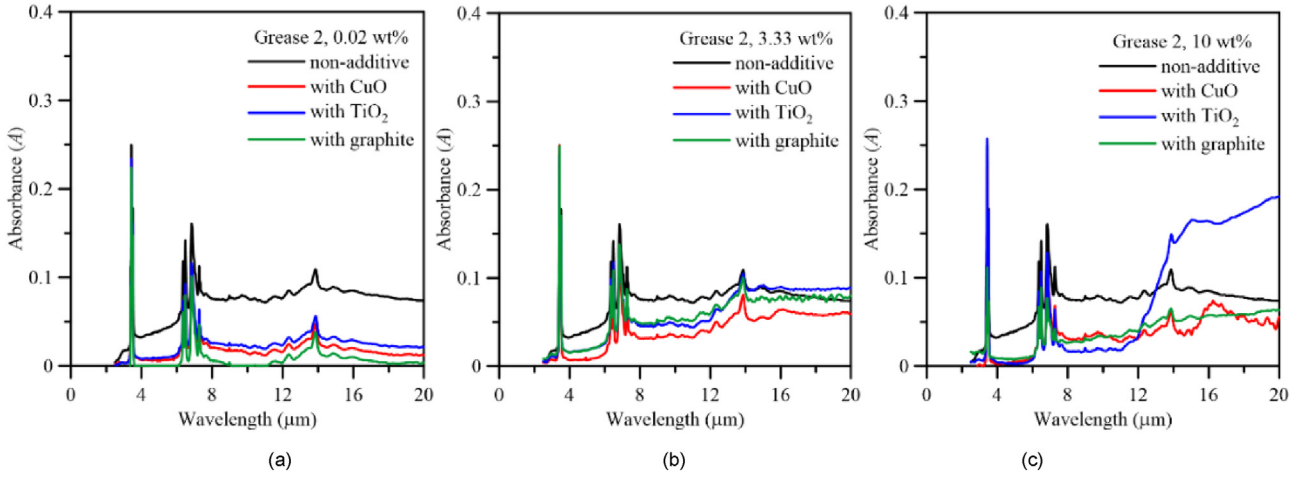


Fig. 7. Absorption measurements for Grease 2, with and without additives: (a) 0.02 wt%; (b) 3.33 wt%; (c) 10 wt%.

DDA method was applied to examine the single-particle effect. We assumed that the sizes of the microparticles, which were diffuse, emitter-absorbers, were the same (D = 2.5 μm) for each additive material. Although the particle size distributions were heterogeneous, and the size of the graphite particles was much larger than for the other materials, an effective particle radius of 2.5 μm was used in our calculations. The sensitivity of orientation averaging was achieved and the results were obtained with a dipole number of $\boldsymbol{N}$ = 433146. The complex refractive indices of the added materials are shown in Table 1. Several values for the m index of copper oxide are given in the literature, and the values for n are in the range 1.8–2.5 [24,25,36]. Since we assumed that all particles were absorber and diffuse, we were able to analyse the effects of the n and k values of the m index on the absorbance and scattering

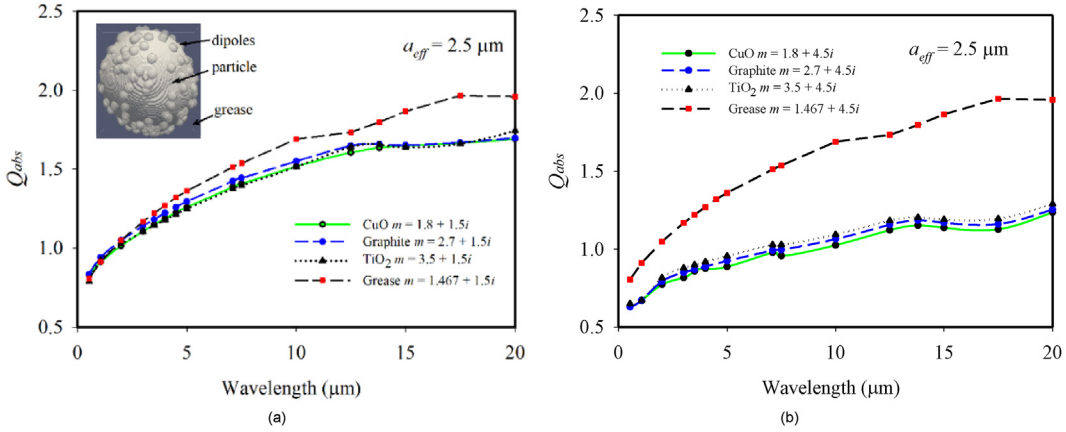


Fig. 8. Comparison between absorbance efficiency results of the grease without and with a particle for different imaginary part: (a) k = 1.5; (b) k = 4.5.

efficiencies, not dependence by wavelength. Initially, to determine the effects of a change in the value of n, we tested all the defined values of n at a constant value of k = 1.5 in the DDA calculations, and found that the results were almost the same. We therefore chose m = 1.8 + 1.5i for CuO, and similar studies were performed for TiO_2 and graphite. In the DDA analysis, the complex refractive index of the grease as the host media needed to be defined, and a value of m = 1.467 was used in these calculations [37]. From an analysis of the effects of a change in the index k, the values of n and k for the metal particles were found to increase with wavelength up to large values, as determined experimentally and numerically by Dombrovsky [38]. A similar effect was reported by Lide [39], in which the n and k values for various metals at wavelengths of 0.589 and 10 μm increased significantly with wavelength. The k values of the m index can also be used to obtain the absorption coefficient (κ), defined as $4\pi k/\lambda_0$ [3]. With the help of all these detailed studies, in order to examine the effects of the k index in our study, the value of k for all the microparticles was taken as 4.5. Fig. 8 shows a comparison of the absorption efficiency factors for two different values of k for the complex refractive indices for greases with and without added microparticles. The changes of the predicted absorption efficiencies of a particle inside the grease were found to be similar to those measured in experimental studies shown in Figs. 6 and 7. When the value of k was high, a ripple structure in the absorption efficiency according to the wavelength as in absorbance measurements can be seen in Fig. 8(b). When the k values were low, the absorption efficiency of the samples increased with the wavelength; however, the dependence of the ripple structure on the wavelength was slight, as shown in Fig. 8(a). In addition, the weak absorption efficiency of the particle indicated that the scattering efficiency was strong.

5. Conclusions

The heat transfer properties of two types of grease were investigated for use in heavy machinery in outdoor environments. The absorption properties of greases with and without additives were experimentally analysed by spectrophotometer measurements. Temperature and torque measurements of the samples were performed using a test rig that was specially prepared for these tests. CuO, TiO2 and graphite microparticles were added to the greases at weight fractions of 0.02, 3.33 and 10 wt%. We can draw the following conclusions from the results of these experimental and numerical studies:

- The temperature distributions of Grease 1 with microparticles were lower than for Grease 1 with no additives, whereas the distributions for Grease 2 with microparticles were higher than for Grease 2 with no additives. Thicker materials were effective on the temperature distributions of the greases.
- The torque values for Grease 1 were lower than for Grease 2 except in the initial period of operation. The torque values for Grease 1 with CuO at 0.02 wt% were the lowest of all the cases studied here.
- For non-additive greases, the absorbance values of Grease 2 were up to 25% higher than for Grease 1 at ~ 0.3 μm.
- When the weight fraction of the added materials was small (≤3.33 wt%), the absorption values for greases with no additives were higher than for those with additives, for both types of grease.
- By using the DDA method and correctly defining k in the complex refractive index, we showed that the absorption properties of a metal particle in the grease increase in the near-infrared wavelength range, as can be seen from the results of absorbance measurements.

We found that the heat transfer properties of the greases with additives were better than those of non-additive greases, based on both temperature and absorption measurements, for use in heavy machinery in outdoor environments.

Declaration of Competing Interest

The authors declare that they have no known competing financial interests or personal relationships that could have appeared to influence the work reported in this paper.

References

[1] Q. Cheng, J. Chai, Z. Zhang, Investigation of double-layer coating pigmented with CuO particles of different concentrations on aesthetic and thermal aspects, Int. J. Therm. Sci. 105 (2016) 36–44, https://doi.org/10.1016/j.ijthermalsci.2016.02.010.
[2] R. Levinson, P. Berdahl, H. Akbari, Solar spectral optical properties of pigments - Part I: Model for deriving scattering and absorption coefficients from transmittance and reflectance measurements, Sol. Energy. Mater. Sol. Cells 89 (4) (2005) 319–349, https://doi.org/10.1016/j.solmat. 2004.11.012.
[3] J. R. Howell, R. Siegel, M. P. Mengüç, Thermal Radiation Heat Transfer fifth ed., CRC Press, Taylor & Francis Group New York, 2010, pages 32, 98.
[4] J.J. Taha-Tijerina, Thermal transport and challenges on nanofluids performance, Microfluidics Nanofluidics 1 (2018) 215–256, https://doi.org/10.5772/intechopen.72505.
[5] M. Kaneta, T. Ogata, Y. Takubo, M. Naka, Effects of a thickener structure on grease elastohydrodynamic lubrication films, Proc. Inst. Mech. Eng. Part J: J. Eng. Tribol. 214 (4) (2000) 327–36. doi: 10.1243/1350650001543214
[6] P.M. Lugt, Grease Lubrication in Rolling Bearings, John Wiley & Sons Ltd, 2012. doi: 10.1002/9781118483961.
[7] M.C. Sánchez, J.M. Franco, C. Valencia, C. Gallegos, F. Urquiola, R. Urchegui, Atomic force microscopy and thermo-rheological characterisation of lubricating greases, Tribol. Lett. 41 (2) (2011) 463–470, https://doi.org/10.1007/s11249-010-9734-x.
[8] B.K. Prasad, S. Rathod, M.S. Yadav, O.P. Modi, Effects of some solid lubricants suspended in oil toward controlling the wear performance of a cast iron, J. Tribol. 132 (4) (2010), https://doi.org/10.1115/1.4002217.
[9] R. Nicoletti, The importance of the heat capacity of lubricants with nanoparticles in the static behavior of journal bearings, J. Tribol. 136 (2014), https://doi.org/10.1115/1.4027861 044502.
[10] D. Goyal, R.K. Dang, S.S. Dhami, A. Chauhan, Effect of nanoparticles based lubricants on static thermal behaviour of journal bearings: a review, Res. J. Eng. Technol. 8 (2017) 149–153, https://doi.org/10.5958/2321-581X017.00.2023.X.
[11] L. Peña-Parás, P. García-Pineda, D. Maldonado-Cortés, G.T. Garza, J. Taha-Tijerina, Temperature dependence of the extreme-pressure behavior of CuO and TiO_2 nanoparticle additives in metal-forming polymeric lubricants, Ind. Lubr. Tribol. 69 (5) (2017) 730–737, https://doi.org/10.1108/ILT-02-2016-0023.
[12] H. Hong, A. Waynick, W. Roy, Heat transfer nanolubricant and nanogrease based on carbon nanotube, ECS Trans. 2 (12) (2007) 133–138, https://doi.org/10.1149/1.2408959.
[13] C.-G. Lee, Y.-J. Hwang, Y.-M. Choi, J.-K. Lee, C. Choi, J.-M. Oh, A study on the tribological characteristics of graphite nano lubricants, Int. J. Precis. Eng. Manuf. 10 (1) (2009) 85–90, https://doi.org/10.1007/s12541-009-0013-4.
[14] R.M. Fikry, R.A. El-Adly, N.A. Ismail, A.S. El-Tabei, H. Al-Aidy, Some azine and azole derivatives as antioxidant additives for lithium lubricating grease, Egypt J. Pet. 22 (1) (2013) 61–71, https://doi.org/10.1016/j.ejpe.2012.07.003.
[15] Y. Zhou, R. Bosman, P.M. Lugt, A model for shear degradation of lithium soap grease at ambient temperature, Tribol. Trans. 61 (1) (2018) 61–70, https://doi.org/10.1080/10402004.2016.1272730.
[16] L. Peña-Parás, J. Taha-Tijerina, A. García, D. Maldonado, A. Nájera, P. Cantú, D. Ortiz, Thermal transport and tribological properties of nanogreases for metal-mechanic applications, Wear 332–333 (2015) 1322–1326, https://doi.org/10.1016/j.wear.2015.01.062.
[17] L. Peña-Parás, H. Gao, D. M. Cortés, A. Vellore, P. García-Pineda, O. E. Montemayor, K. L. Nava, A. Martini, Effects of substrate surface roughness and nano/micro particle additive size on friction and wear in lubricated sliding, Tribol. Int. 119 (2018) 88–98. https://doi.org/10.1016/j.triboint.2017.09.009
[18] L. Hongtao, J. Hongmin, H. Haiping, H. Younes, Tribological properties of carbon nanotube grease, Ind. Lubric. Tribol. 66 (5) (2014) 579–583, https://doi.org/10.1108/ILT-08-2012-0071.
[19] J.P. Ajithkumar, M. Anthony Xavior, Influence of nano lubrication in machining operations—a review, Mater. Today Proc. 5 (5) (2018) 11185–11192, https://doi.org/10.1016/j.matpr.2018.01.142.
[20] R. Kandasamy, I. Muhaimin, R. Mohamad, Thermophoresis and Brownian motion effects on MHD boundary-layer flow of a nanofluid in the presence of thermal stratification due to solar radiation, Int. J. Mech. Sci. 70 (2013) 146–154, https://doi.org/10.1016/j.ijmecsci.2013.03.007.

[21] N. Wang, G. Xu, S. Li, X. Zhang, Thermal properties and solar collection characteristics of oil-based nanofluids with low graphene concentration, Energy Procedia 105 (2017) 194–199, https://doi.org/10.1016/j.egypro.2017.03.301.
[22] S. Ahlatli, T. Mare, P. Estelle, N. Doner, Thermal performance of carbon nanotube nanofluids in solar microchannel collectors: an experimental study, Int. J. Technol. (IJTech) 2 (2016) 78–85. https://doi.org/10.14716/ijtech.v7i2.1575.
[23] N. Doner, A.R. Pargan, A. Aygahoglu, F. Liu, F. Sen, Radiative properties of hematite particles in the UV-visible spectrum, Int. J. Therm. Sci. 139 (2019) 79–87, https://doi.org/10.1016/j.ijthermalsci.2019.02.006.
[24] V. Usha, S. Kalyanaraman, R. Thangavel, R. Vettumperumal, Effect of catalysts on the synthesis of CuO nanoparticles: Structural and optical properties by sol-gel method, Superlatt. Microstruct. 86 (2015) 203–210, https://doi.org/10.1016/j.spmi.2015.07.053.
[25] K.M. Shrestha, C.M. Sorensen, K.J. Klabunde, Synthesis of CuO nanorods, reduction of CuO into Cu nanorods, and diffuse reflectance measurements of CuO and Cu nanomaterials in the near infrared region, J. Phys. Chem. C 114 (34) (2010) 14368–14376, https://doi.org/10.1021/jp103761h.
[26] Y. Hwang, J.K. Lee, C.H. Lee, Y.M. Jung, S.I. Cheong, C.G. Lee, B.C. Ku, S.P. Jang, Stability and thermal conductivity characteristics of nanofluids, Thermochim. Acta 455 (1–2) (2007) 70–74, https://doi.org/10.1016/j.tca.2006.11.036.
[27] L.E. McNeil, R.H. French, Multiple scattering from rutile TiO_2 particles, Acta Mater. 48 (18-19) (2000) 4571–4576, https://doi.org/10.1016/S1359-6454(00)00243-3.
[28] J.G. Speight, Lange's Handbook of Chemistry, 16th ed., McGraw-Hill Inc, New York, 2004, p. 1608.
[29] L.X. Ma, J.Y. Tan, J.M. Zhao, F.Q. Wang, C.A. Wang, Y.Y. Wang, Dependent scattering and absorption by densely packed discrete spherical particles: effects of complex refractive index, J. Quant. Spectrosc. Radiat. Transf. 196 (2017) 94–102, https://doi.org/10.1016/j.jqsrt.2017.03.039.
[30] S.H. Kim, S.R. Choi, D. Kim, Thermal conductivity of metal-oxide nanofluids: Particle size dependence and effect of laser irradiation, J. Heat Trans. 129 (3) (2006) 298–307, https://doi.org/10.1115/1.2427071.
[31] B.T. Draine, P.J. Flatau, Discrete-dipole approximation for scattering calculations, J. Opt. Soc. Am. A. 11 (4) (1994) 1491–1499, https://doi.org/10.1364/JOSAA.11.001491.
[32] I. Ayrancı, R. Vaillon, N. Selçuk, Performance of discrete dipole approximation for prediction of amplitude and phase of electromagnetic scattering by particles, J. Quant. Spectrosc. Radiat. Transf. 103 (1) (2007) 83–101, https://doi.org/10.1016/j.jqsrt.2006.06.006.
[33] B. T. Drain, F. J. Piotr, User guide for the discrete dipole approximation code DDSCAT 7.3. arXiv preprint arXiv 81. https://www.researchgate.net/publication/45899844_User_Guide_for_the_Discrete_Dipole_Approximation_Code_DDSCAT_73 (2013).
[34] Y. Kanazawa, R.S. Sayles, A. Kadiric, Film formation and friction in grease lubricated rolling-sliding non-conformal contacts, Tribol. Int. 109 (2017) 505–518, https://doi.org/10.1016/j.triboint.2017.01.026.
[35] H. Fredriksson, T. Pakizeh, M. Käll, B. Kasemo, D. Chakarov, Resonant optical absorption in graphite nanostructures, J. Opt. A. Pure Appl. Opt. 11 (2009), https://doi.org/10.1016/j.triboint.2017.01.026.
[36] D. Tahir, S. Tougaard, Electronic and optical properties of Cu, CuO and Cu 2O studied by electron spectroscopy, J. Phys. Condens. Matter. 24 (17) (2012) 175002, https://doi.org/10.1088/0953-8984/24/17/175002.
[37] O. Marklund, L. Gustafsson, Correction for pressure dependence of the refractive index in measurements of lubricant film thickness with image analysis, Proc. Inst. Mech. Eng. Part J J. Eng. Tribol. 213 (2) (1999) 109–126, https://doi.org/10.1243/1350650991542875.
[38] L.A. Dombrovsky, Radiative properties of metal particles in infrared and microwave spectral ranges, Thermopedia (2010), https://doi.org/10.1615/thermopedia.000150.
[39] D.R. Lide, Handbook of Chemistry and Physics, 84th Ed., CRC Press, Boca Roan, 2008.
[40] X. Xi, D.D.L. Chung, Pyropermittivity and pyroelectret behavior of graphite, Carbon 174 (2021) 357–367, https://doi.org/10.1016/j.carbon.2020.12.022.